AGU PUBLICATIONS

JGR

Journal of Geophysical Research: Solid Earth

RESEARCH ARTICLE
10.1002/2015JB011937

Key Points:
- Possible tidal periodicities might be expected due to random chance
- There is no clear tidal triggering signal prior to the 2011 Tohoku EQ

Supporting Information:
- Figures S1–S4

Correspondence to:
W. Wang,
weiwang053@gmail.com

Citation:
Wang, W., and P. M. Shearer (2015), No clear evidence for localized tidal periodicities in earthquakes in the central Japan region, *J. Geophys. Res. Solid Earth*, *120*, 6317–6328, doi:10.1002/2015JB011937.

Received 11 FEB 2015
Accepted 4 AUG 2015
Accepted article online 6 AUG 2015
Published online 15 SEP 2015

No clear evidence for localized tidal periodicities in earthquakes in the central Japan region

W. Wang[1] and P. M. Shearer[1]

[1]Scripps Institution of Oceanography, University of California, San Diego, La Jolla, California, USA

Abstract We search for possible localized tidal triggering in earthquake occurrence near Japan by testing for tidal periodicities in seismicity within a variety of space/time bins. We examine 74,610 earthquakes of $M \geq 3$ in the Japan Meteorological Agency catalog from January 2000 to April 2013. Because we use many earthquakes for which accurate focal mechanisms are not available, we do not compute tidal stresses on individual fault planes but instead assume that the mechanisms are likely to be similar enough among nearby events that tidal triggering will promote earthquake occurrence at specific tidal phases. After dividing the data into cells at a range of spatial (0.2°, 0.5°, and 1.0°) and temporal dimensions (100, 200, and 400 days), we apply Schuster's test for nonrandom event occurrence with respect to both the semidiurnal and semimonthly tidal phases. Because the resulting p values will be biased by temporal clustering caused by aftershocks, we apply a declustering method that retains only one event per tidal cycle per phase increment. Our results show a wide range of p values for the localized earthquake bins, but the number of bins with very small p values (e.g., $p < 0.05$) is no more than might be expected due to random chance, and there is no correlation of low p value bins with the time of the 2010 M 9.0 Tohoku-Oki earthquake.

1. Introduction

Because cyclical stressing rates from the Earth tides are typically much higher than the long-term buildup rate of tectonic stresses, many studies have searched for a possible correlation between earthquake occurrence and tidal phase. Although most of these studies find no clear relation between earthquakes and tides, evidence for at least some correlation has been found in a number of regions. *Métivier et al.* [2009] and *Wilcock* [2009] reported regional tidal triggering, and *Tanaka et al.* [2002a, 2002b] and *Cochran et al.* [2004] reported tidal triggering influence on a global scale. Some studies have reported a positive correlation between tidal triggering and certain types of focal mechanisms [*Tsuruoka et al.*, 1995; *Cochran et al.*, 2004]. On the other hand, *Shudde and Barr* [1977] and *Vidale et al.* [1998] reported no correlation or a weak regional correlation, and, on a global scale, *Heaton* [1982] and *Hartzell and Heaton* [1989] found no evidence for tidal triggering.

Recently, *Tanaka* [2010, 2012] suggested that enhanced tidal correlation of earthquake occurrence may occur prior to large earthquakes in a region near their hypocenters, including recent giant megathrust earthquakes in Sumatra and Japan. Motivated in part by these results, *Brinkman et al.* [2015] presented an earthquake generation model that predicts an increased likelihood of large earthquakes during periods when small earthquake occurrence correlates with daily tidal stresses. Because of the potential value of Tanaka's observations for earthquake prediction, it is important to see if they can be confirmed using additional data. Her analyses for the 2004 Sumatra and 2011 Tohoku-Oki earthquakes used the Global Centroid Moment Tensor (GCMT) catalog [*Tanaka*, 2010, 2012] of $M \geq 5$ events. Here we take advantage of the much larger catalog of Japanese events provided by the local networks to examine possible localized tidal triggering of earthquakes near Japan, including time periods before and after the 2011 M_w 9.0 Tohoku-Oki earthquake. We find no clear evidence for statistically significant tidal periodicities in the seismicity rate for any of our space-time seismicity bins.

2. Method

Ideally, studies of possible tidal triggering of earthquakes should compute the tidal stresses on the earthquake faults to establish directly when earthquakes should be encouraged and discouraged. This requires knowledge of the fault orientation, which is usually estimated from focal mechanisms and the local

tectonics. However, because event catalogs typically only include focal mechanisms for relatively large earthquakes, this prevents analysis of the much more numerous smaller events.

Here we adopt the simpler approach of searching for nonrandom distributions of event times with respect to tidal phase, without establishing any explicit relationship to stress or the most likely tidal phase to promote triggering. It should be noted that this approach could fail to detect tidal triggering if a variety of focal mechanisms are present in a region, which trigger at different times during the tidal cycle. However, because nearby events typically have similar focal mechanisms [e.g., *Hardebeck*, 2006], it is likely that sufficiently localized regions will show clear peaks in occurrence time phase if tidal triggering is present. That is, similar mechanisms likely have similar fault orientations and will have similar tidal stress behavior on the fault and thus should trigger at nearly the same tidal phase. If local tidal triggering is present, we should then see a peak in the number of events occurring at a particular tidal phase rather than a purely random distribution of tidal phases.

To test the local similarity of Japanese focal mechanisms, we use events from the 1990 to 2010 GCMT catalog (see Figure 1) and apply *Hardebeck*'s [2006] method to measure the angular difference between focal mechanism pairs. The angular difference is defined as the minimum rotation about any axis to bring the two mechanisms into alignment. Figure 2 shows the relation between the hypocentroidal distance separation and angular difference of each pair of events in the GCMT catalog. There is large scatter, but, as expected, the median angular difference decreases as the separation distance decreases. Very similar results are obtained using the declustered catalog that we describe later. The median angular difference is 31.0°, 41.6°, and 48.3° for separation distances of 0.2°, 0.5°, and 1°, respectively. However, given that the median angular difference is about 20° even at zero separation, it is likely that a substantial fraction of the observed angular differences are due to measurement error, rather than true differences in mechanisms [see *Hardebeck*, 2006]. In any case, our approach here is to focus on nearby events for which our assumption of focal mechanism similarity is most likely to be valid. We therefore experiment with dividing the data into cells with spatial scales of 0.2°, 0.5°, and 1.0°. To test for possible temporal variations in tidal triggering, we also divide the data into temporal cells of 100 days, 200 days, and 400 days, aligned with the Tohoku-Oki earthquake time to account for the possibility of abrupt changes at the time of this earthquake.

For the seismicity in each space-time cell, we apply Schuster's test (often used in tidal triggering studies, e.g., *Schuster* [1897], *Heaton* [1982], and *Tanaka et al.* [2002a, 2002b, 2006]) to test for statistically significant nonrandom distributions of tidal phases at the event times. Earth tides exhibit a variety of periodicities, but two of the strongest are the semidiurnal (12.4206 h period) and the semimonthly (14.7653 day period). Note that the semimonthly period is the average time between new and full Moons, when the tides have higher amplitudes due to the beating between the periods of the lunar and solar tides. If earthquakes are quickly triggered at a threshold maximum level of stress, then both of these periods are likely to be associated with earthquake occurrence.

For these two periods, we compute p values for the distribution of tidal phases using

$$p = \exp\left(-\frac{\left(\sum_{i=1}^{N}\cos\theta_i\right)^2 + \left(\sum_{i=1}^{N}\sin\theta_i\right)^2}{N}\right) \quad (1)$$

where N is the number of earthquakes in the cell and θ_i is the tidal phase of the ith event. The p value is an estimate of the probability that the tidal phases are randomly distributed; thus, $p < 5\%$ indicates a possibly significant correlation between Earth tide and earthquake occurrence in the cell.

As discussed before, we have divided the catalog into small cells and apply Schuster's test separately to the data in each cell. Because there are a large number of cells, about 5% of them are expected to have p values smaller than 0.05 purely by random chance. However, if localized tidal triggering is present for a significant number of cells, the number of cells with $p < 0.05$ will be above the expected average. We test for this by plotting histograms of the p values at increments of 0.05, compared to a reference line that shows the expected purely random distribution.

Schuster's test assumes that earthquakes are independent events, and thus, the p values can be biased by temporal earthquake clustering unrelated to the tides (e.g., aftershock sequences). We can test whether this is an important factor in our data set by examining the distributions of p values for periods not associated with

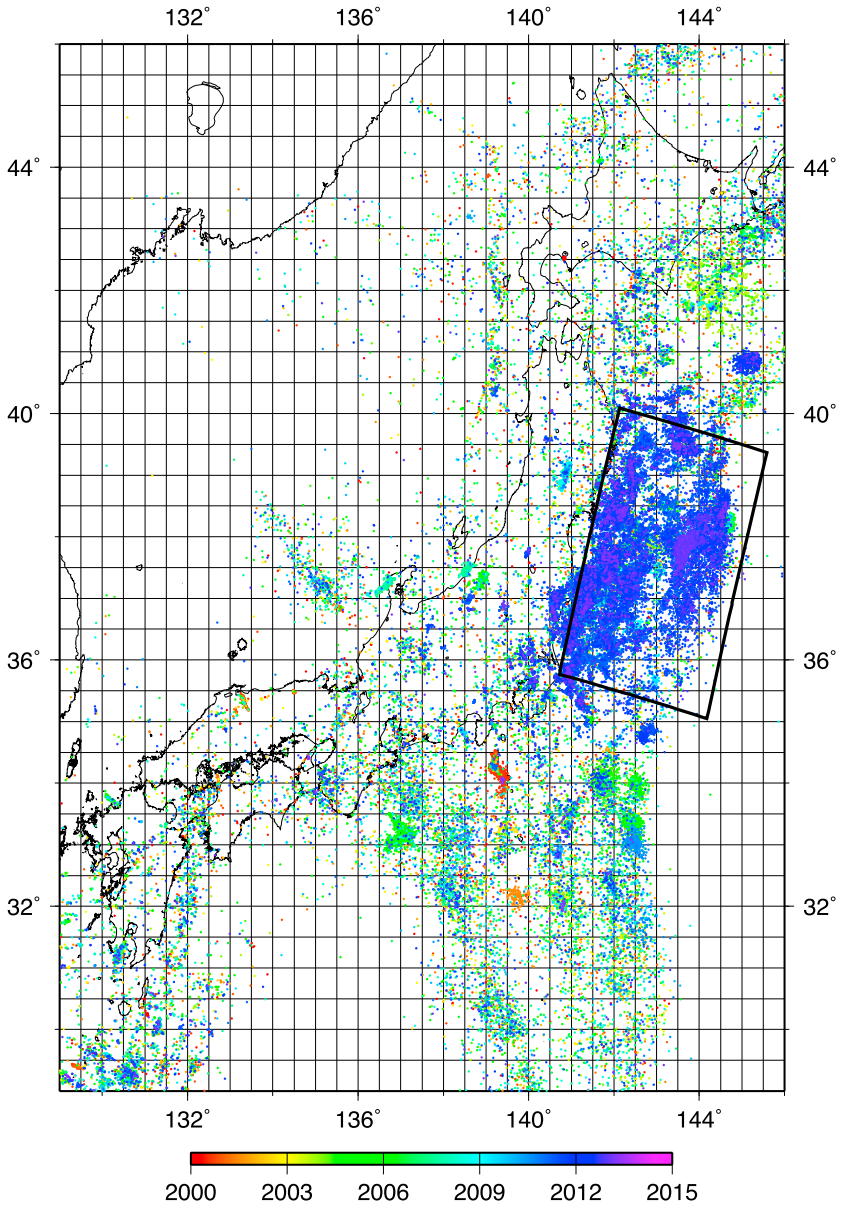

Figure 1. Earthquakes used in this study. The 74,610 events of $M_w \geq 3.0$ from the JMA catalog (January 2000 to April 2013) are plotted, colored by their year of occurrence. Grid lines are shown every 0.5°.

the tides, i.e., for which no triggering should be detected. For this purpose we use over 70,000 earthquakes from the Japan Meteorological Agency (JMA) catalog (see next section for more details) and test over 500 seismicity bins at increments of 0.5° and 200 days. We first analyze the raw catalog and test for nonrandom phase by computing the *p* values with respect to periods of 7 h, 12.42 h (the semidiurnal tidal period), and 17 h, as well as the much longer periods of 11 days, 14.77 days (the semimonthly tidal period), and 19 days. These results are plotted in the left column of Figure 3, which includes only bins for which there are 10 or more events. In all cases, there are many more bins with *p* values less than 0.05 than would be expected due to random chance, and this is just as true for the nontidal periods as the tidal periods. This is strong evidence that temporal clustering is biasing the results.

Because most of the temporal clustering is probably caused by aftershock sequences, we first experimented with removing aftershocks by applying the Reasenberg Declustering Method (RDM) [*Reasenberg*, 1985]. The basic idea of RDM is to identify aftershock populations by defining an interaction zone following each earthquake in the catalog. Any earthquake that occurs within the interaction zone of a prior earthquake is

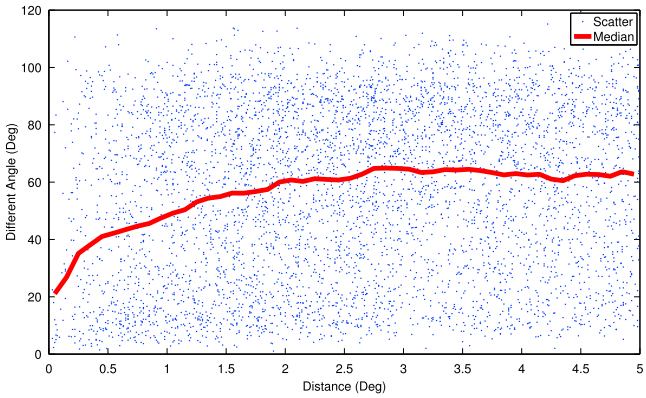

Figure 2. The angular difference between GCMT focal mechanisms versus their interhypocentral distance for event pairs in our study region. The red line is the median, computed in bins at 0.1° spaces. For clarity only a random 1% of the points are plotted.

considered an aftershock and is statistically dependent on it. Events thus associated are referred to as belonging to a cluster. The spatial and temporal extents of the interaction zone increase with the main shock size and are defined based on a probabilistic model. We applied the RDM algorithm (using its default parameters) to the complete catalog to remove likely aftershocks and then processed the declustered catalog using the same binning scheme as before. These results are shown in Figure 3 (middle column). The anomalously large number of p values below 0.05 is reduced somewhat compared to the raw catalog, particular for the shorter periods shown in Figure 3a. However, with the exception of the results for the 7 h period, there are still more anomalous p values than expected due to random chance, even for the nontidal periods. By increasing the radius scaling in the Reasenberg method one can remove slightly more events, but not enough to change the overall results shown in Figure 3. Thus, the RDM approach does not seem to assure statistical independence of the occurrence times that go into Schuster's test.

This could be caused by several factors. RDM may not be removing all the aftershocks, or the catalog could have a significant number of swarms, which have temporal clustering but are not readily explained with main shock-to-aftershock triggering. To better remove the biasing effects of temporal clustering, we develop a new approach to event declustering that is specific to tidal triggering analysis. This method bins the seismicity within each cell into 16 equal increments of tidal phase and retains only the maximum-sized earthquake per phase increment per tidal cycle number (see Figure 4). This prevents a large number of events separated in time by only a small fraction of the target tidal periodicity from biasing the results. It also has the advantage of potentially being able to identify tidal periodicities within extended aftershock sequences (i.e., spanning many tidal cycles), which contain mostly events that would be removed with RDM declustering. Results of applying this tidal phase binning approach are shown in Figure 3 (right column). The distribution of p values now appears much more random, both at tidal periods and the four other periods that we tested.

Note that if tidal periodicities are present in a data set, the phase binning approach is slightly more likely to remove periodic events than "background" random events because they are more likely to occur in the same phase bin. However, this bias is small, provided the number of tidal cycles is large, and we ignore its effects here. Another potential difficulty with this approach would occur if the seismicity rates were so high that most of the potential time bins contained earthquakes, in which case tidal periodicity might appear only as a larger number of events within particular bins and would go undetected if only one event is retained per bin. However, in our analyses generally only a small fraction of the phase bins contains earthquakes. In particular, 99.7% of our tests for semidiurnal tides and 85.5% of our tests for semimonthly tides have events in fewer than 20% of the phase bins. Thus, this is not a problem for the vast majority of our tests, with most of the exceptions being for the semimonthly tests during the very high seismicity rate immediately following the Tohoku main shock. Because the tidal phase binning approach provides the least biased results, we adopt this method for the remainder of our analyses.

To see how our approach compares to more established methods for analyzing tidal triggering based on Coulomb stress changes [e.g., *Vidale et al.*, 1998], we examined solid Earth tidal strains (including the ocean loading term) computed for the Tohoku-Oki earthquake region from 2005 through 2007 (D. Agnew,

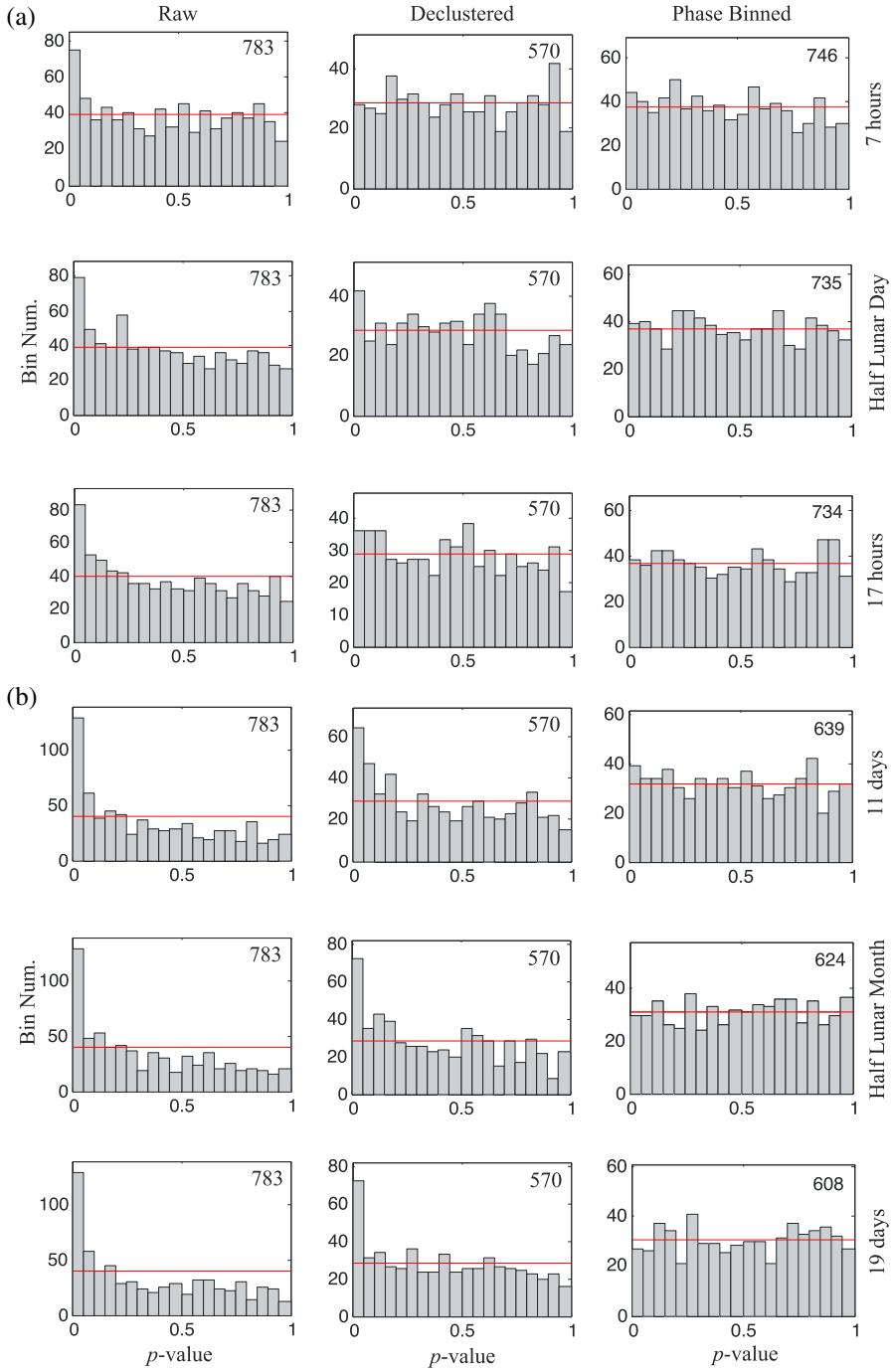

Figure 3. (a and b) A comparison of the *p* value distribution resulting from periodicity tests applied to seismicity bins in (left column) the original JMA catalog, (middle column) the Reasenberg declustered catalog, and (right column) the phase bin declustered catalog. The histograms show the numbers of *p* values for bins with cell dimension (0.5° and 200 days) for tests at different possible periods, including nontidal and tidal. The number in the upper right corner shows the total cell numbers for each case. The red line shows the expected number for a purely random distribution.

personal communication, 2015). We compared the strains at three different offshore points but saw only very small differences among them, so for simplicity we consider only a point (36.54°N, 141.77°E) near the Tohoku epicenter. We do not take into account earthquake depth in the strain calculation, but there is little depth dependence in the strain within the crust. From the strain tensor, we compute the stress tensor components assuming $\lambda = 45.9$ GPa and $\mu = 44.1$ GPa. We assume a large background tectonic stress (20 MPa) with

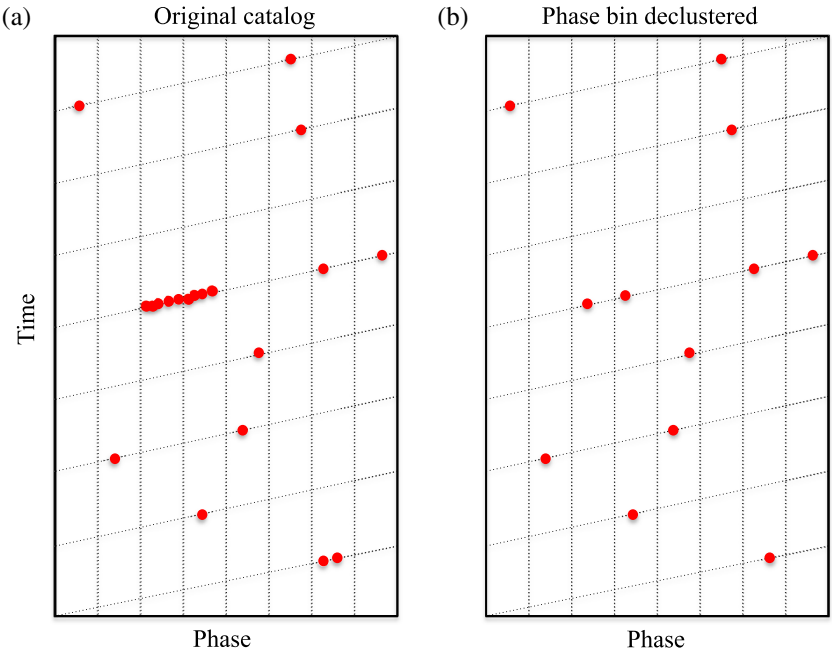

Figure 4. A synthetic example showing how the phase bin declustering method works. (a) Event time versus phase for a given period. Red dots represent individual event locations in time versus phase. Vertical dashed lines separate each cycle into eight equal increments. The sloping lines show increasing phase with respect to time in each cycle. Note that events within a tight temporal cluster (e.g., a swarm or aftershock sequence) will tend to occur at the same phase, possibly biasing tests of phase randomness. (b) The phase bin declustered catalog, in which only the maximum magnitude event is retained for each phase bin at each cycle.

horizontal convergence at 293°N, i.e., perpendicular to the trench. This allows us to compute the Coulomb stress changes [e.g., *King et al.*, 1994] for faults of any orientation assuming an effective coefficient of friction of 0.4. For the shallow-dipping fault plane (strike 203°, dip 10°) inferred from the main shock GCMT solution, these stresses have daily maximum values of about 2700 Pa during the times of new Moon and full Moon, and maximum values of about 700 Pa during first quarter Moon and third quarter Moon.

We then performed two different tests. For the first test, we assumed the fault orientation of the GCMT solution for the Tohoku main shock and computed the Coulomb stress as a function of time. We then found a stress value that is exceeded for only 5% of the time and created a series of synthetic catalogs of n events with times randomly assigned within these periods of high Coulomb stress. For each random catalog, we applied Schuster's test for both the semidiurnal and semimonthly periods and computed p values. For $n = 20$, we found that 100% of the catalogs had p values below 0.05 for the semidiurnal period and 50% had p values below 0.05 for the semimonthly period. For the second test, we assigned a random fault orientation to each event, computed the Coulomb stress, and assigned a random time from within the 5% of the time with maximum stress. As expected for random fault orientations, the resulting event times are less obviously periodic. For $n = 20$, we found that only 10% of the catalogs had p values below 0.05 for the semidiurnal period and 15% had p values below 0.05 for the semimonthly period. The fraction of significant p values increases with the number of events in the synthetic catalog. For $n = 100$, 30% of the catalogs had p values below 0.05 for the semidiurnal period and 56% had p values below 0.05 for the semimonthly period. Thus, given sufficient numbers of events, our simple approach will detect tidal triggering driven by Coulomb stress changes, even if the faults have random orientation. However, as described above and shown in Figure 2, the focal mechanisms in our data set are quite similar over short distances, and thus, we expect our method to perform for the real data more like the first synthetic test than the second. Our test is less sensitive than tests based on explicit Coulomb stress calculations because we do not take into account the tidal stress amplitude (e.g., some of the 12 h tides are of higher amplitude than others). However, because we do not require event focal mechanisms, we can apply our test to larger numbers of events, which should compensate to some degree for its lower sensitivity.

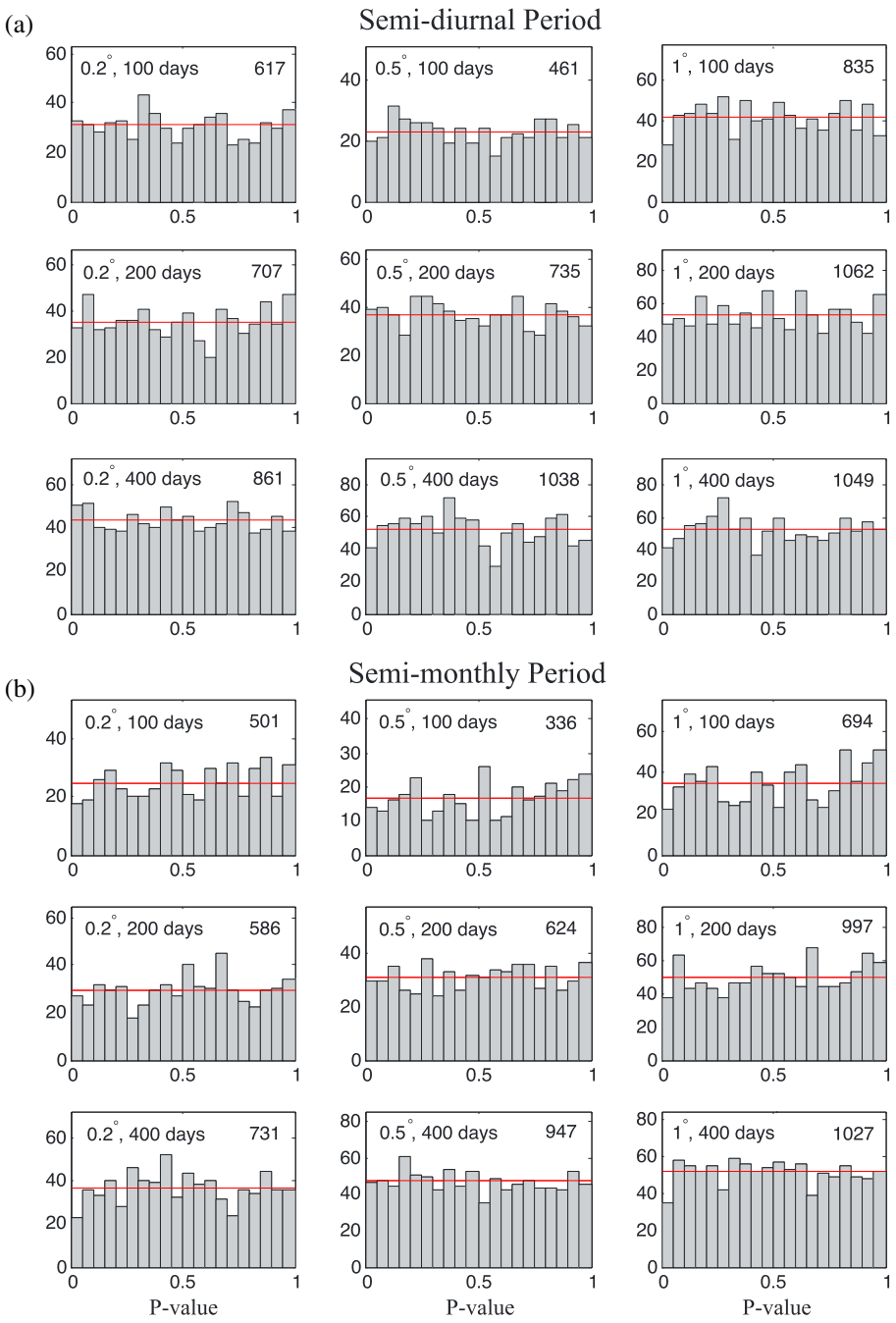

Figure 5. Histograms of the *p* value distributions for tests of seismicity periodicity for (a) the semidiurnal tidal period and (b) the semimonthly tidal period, for bins over a range of spatial (0.2°, 0.5°, and 1.0°) and temporal dimensions (100, 200, and 400 days). The numbers in the upper left corner show "spatial, temporal, and size" for each case. The number in the upper right corner in each histogram shows the total number of cells. The red line shows the expected number for a purely random distribution.

3. Results

We examine $M \geq 3$ events in the JMA catalog from January 2000 to April 2013 in the central Japan region from 130°E to 146°E and from 29°N to 46°N (see Figure 1). Although the JMA catalog contains many events smaller than M 3, we use this cutoff to yield a relatively complete catalog even in the offshore region (see supporting information Figure S1). It is possible that the catalog is missing a small number of events larger

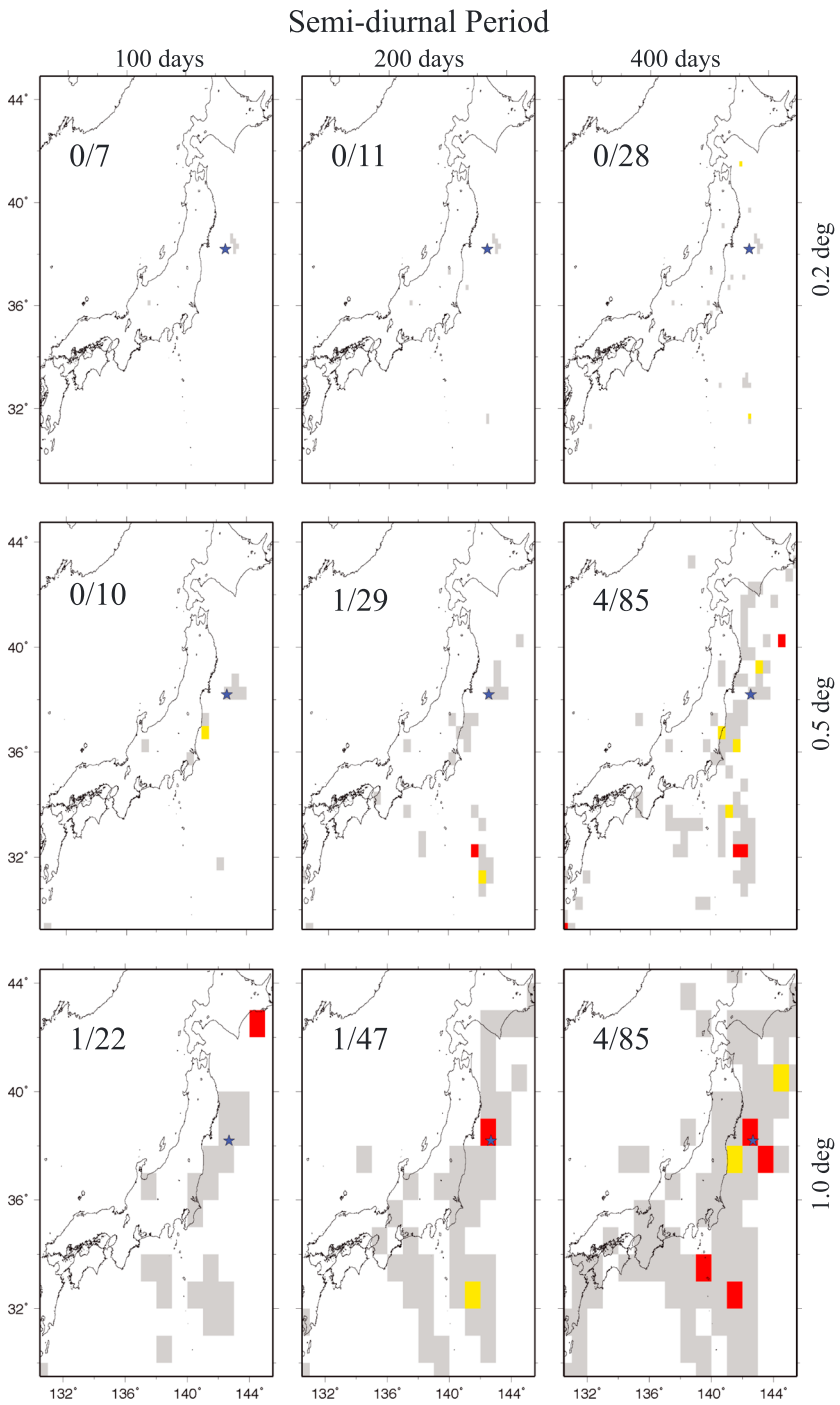

Figure 6. The spatial distribution of anomalous *p* values for possible semidiurnal tidal periodicity for $M \geq 3$ seismicity bins over a range of spatial (0.2°, 0.5°, and 1.0°) and temporal dimensions (100, 200, and 400 days), with each time bin ending immediately before the 2011 M_w 9.0 Tohoku-Oki earthquake. The star indicates the main shock epicenter from *Chu et al.* [2011]. Red indicates *p* values less than 0.05, yellow for *p* values between 0.05 and 0.1, and gray for the other *p* values. Only cells with more than 10 events are plotted. The number in each panel shows "(number of cells with $p < 0.05$)/(number of plotted cells)."

than *M* 3, but this is unlikely to bias our results very much, particularly because there is no reason to expect tidally triggered events to be absent from the catalog more than nontidally triggered events. Later we will show that our results are robust with respect to the minimum magnitude; i.e., we obtain similar conclusions using a less conservative *M* 2.5 cutoff. We analyze a total of 74,610 earthquakes, of which only 1187 are in

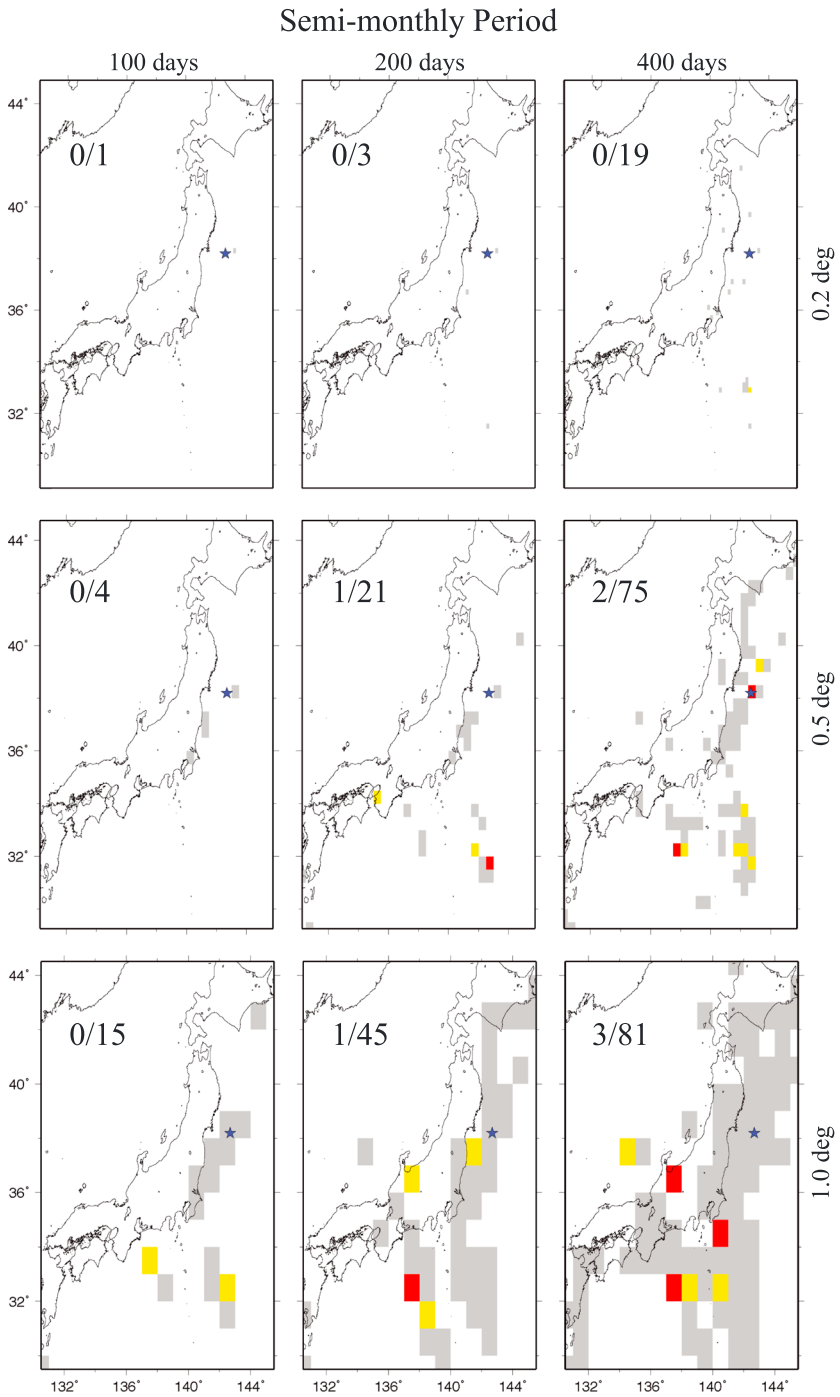

Figure 7. The spatial distribution of anomalous *p* values for possible semimonthly tidal periodicity for $M \geq 3$ seismicity bins over a range of spatial (0.2°, 0.5°, and 1.0°) and temporal dimensions (100, 200, and 400 days), with each time bin ending immediately before the 2011 M_w 9.0 Tohoku-Oki earthquake. The star indicates the main shock epicenter from *Chu et al.* [2011]. Red indicates *p* values less than 0.05, yellow for *p* values between 0.05 and 0.1, and gray for the other *p* values. Only cells with more than 10 events are plotted. The number in each panel shows (number of cells with $p < 0.05$)/(number of plotted cells).

the GCMT catalog, with 25 earthquakes larger than *M* 7.0 including the 2011 M_w 9.0 Tohoku-Oki earthquake. We divide the data into cells with a range of spatial (0.2°, 0.5°, and 1.0° in both latitude and longitude) and temporal dimensions (100, 200, and 400 days) and compute the *p* value for each cell (following our phase bin declustering method) with respect to both the semidiurnal and semimonthly tidal phases.

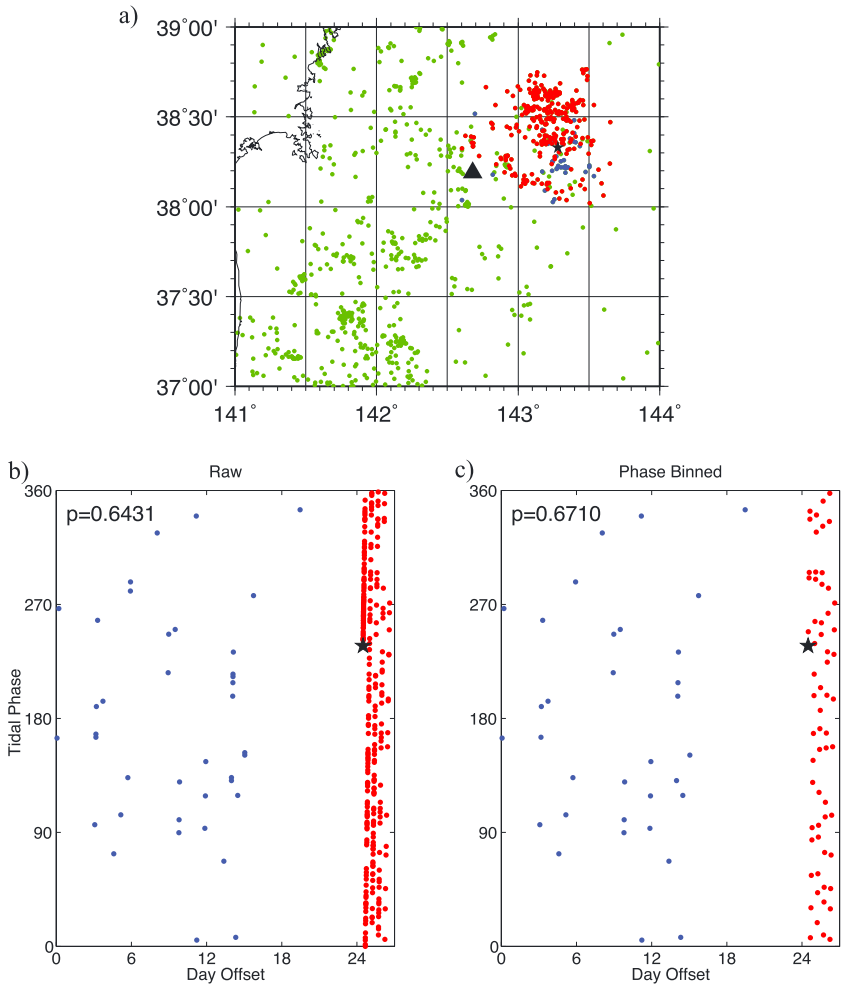

Figure 8. Foreshocks of the Tohoku-Oki earthquake: (a) Map of seismicity in the foreshock region within 400 days prior to the M_w 9.0 Tohoku-Oki earthquake, showing the epicenters of the M_w 9.0 main shock (large black triangle) and the M_w 7.3 foreshock (small black star) and all the 327 $M_w \geq 2.5$ foreshocks (blue and red dots) between 13 February 2011 and 11 March 2011, including aftershocks of the M_w 7.3 foreshock (red dots). (b) Diurnal tidal phase versus time for the original 23 day foreshock sequence of the Tohoku-Oki earthquake between 13 February 2011 and 11 March 2011. Black star represents the M_w 7.3 foreshock, and the p value is listed. (c) Diurnal tidal phase versus time for the phase bin declustered 23 day foreshock sequence of the Tohoku-Oki earthquake between 13 February 2011 and 11 March 2011.

Figure 5 summarizes our results for all of the space-time bins with respect to both the semidiurnal and semimonthly tidal phases, presenting results only for bins containing at least 10 events. The distribution of p values now appears close to random. Although one can identify specific bins with p values below 0.05, the total number of such bins is close to what would be expected due to random chance. For the semidiurnal tidal period, only three of the nine bin combinations have numbers of p values below 0.05 that are more than the numbers expected due to random chance. For the semimonthly tidal period, none of the nine bin combinations have numbers of p values below 0.05 that are more than the expected numbers. However, this plot could mask the presence of extremely anomalous p values that might nonetheless indicate strong tidal triggering in one or more bins. To test for this possibility, we identified 62 out of 7365 total bins (i.e., 0.84%) with p values less than 0.01 and 2 out of 7365 total bins (i.e., 0.03%) with p values less than 0.001 for semidiurnal tides and for semimonthly tides 37 out of 6443 total bins (i.e., 0.57%) with p values less than 0.01 and none with p values less than 0.001. These numbers do not indicate the presence of any bins with p values below what might be expected for the total number of bins that we analyzed. To test whether these results depend upon the phase bin declustering increment, we repeated our analysis using 8 phase bins instead of 16 and obtained similar results (see supporting information Figure S2).

Tanaka [2010, 2012] suggested that enhanced tidal correlation of earthquakes may occur prior to large earthquakes in a region near their hypocenters. Our results here are relevant to the question as to whether such enhanced tidal correlation can observed before the 2011 M_w 9.0 Tohoku-Oki earthquake. Figures 6 and 7 show the distribution of anomalously low p values (≤ 0.05) for our temporal cells immediately prior to the Tohoku-Oki earthquake. We also plot the *Chu et al.* [2011] hypocenter for the main shock. Red rectangles indicate that the p value of the cell is smaller than 0.05; gray rectangles are for larger p values. In general, the number of cells with $p \leq 0.05$ is no more than would be expected from random chance. There also is no compelling correlation of the red cells in this figure with the Tohoku-Oki epicenter. There are some red cells near the epicenter for the (1°, 200 day) and (1°, 400 day) bins for the semidiurnal period and the (0.5°, 400 day) bin for the semimonthly period (with p values of 0.029, 0.045, and 0.01, respectively), but these anomalies are not robust with respect to the binning scheme. As an additional test, we repeated our analyses using a magnitude cutoff of 2.5 rather than 3.0 (resulting in about 2 times more earthquakes in total) and found that only the (1°, 400 day) semidiurnal bin near the epicenter remained anomalous (in this case with a p value of 0.026 rather than 0.01). The $M \geq 2.5$ results are plotted in supporting information Figures S3 and S4. The $M \geq 2.5$ results also yielded a semidiurnal 0.2° bin near the epicenter with a p value of 0.036 for all three time windows as the 11 events in this bin are all within 100 days of the Tohoku-Oki main shock. The largest occupation fraction of phase bins is 8.54% for the 100 day case. It should be noted that 10 of these 11 events are from the immediate foreshock sequence of the Tohoku-Oki main shock (see below) but represent only a somewhat arbitrarily windowed portion of the complete foreshock sequence.

The Tohoku-Oki earthquake was preceded by a pronounced 23 day foreshock sequence [e.g., *Kato et al.*, 2012], including aftershocks of a M_w 7.3 earthquake occurring 2 days before the M_w 9.0 main shock. The foreshocks occurred mainly to the east and northeast of the main shock epicenter. Because none of our spatial bins captures the entire foreshock sequence, it makes sense to study the sequence separately to see whether it might exhibit any tidal periodicity. Figure 8 shows the locations of 327 $M \geq 2.5$ foreshocks and the diurnal tidal phase versus time for both the raw catalog and the phase bin reclustered catalog (the foreshock sequence is not long enough to test for semimonthly periodicity). The p values in both cases are about 0.65, and thus, there is no evidence for tidal periodicity in the foreshock sequence. Overall, we find no clear evidence for observable tidal triggering in seismicity prior to the 2011 Tohoku-Oki earthquake.

As described earlier, our approach has the advantage of including many more earthquakes than methods that require fault orientations in order to explicitly compute tidal contributions to Coulomb stresses but the disadvantage of not taking into account variations in tidal stress amplitudes. A full Coulomb stress analysis is beyond the scope of our paper, but as a final test we did find the number of events in the catalog from 2005 to 2007 within the 5% of times with the highest Coulomb stress and the 5% of times with the lowest Coulomb stress, assuming all the faults have the same orientation as the shallow-dipping fault in the GCMT solution for the Tohoku main shock. For the Reasenberg declustered catalog, 4.56% and 5.26% of the events occurred during the highest and lowest stress times, respectively. For the original catalog, the corresponding numbers are 4.64% and 5.41%. Thus, these results do not provide any evidence for strong tidal triggering in the 2005–2007 catalog, at least for events with shallow-dipping thrust mechanisms.

4. Conclusions

We use a large set of earthquakes to search for evidence of localized tidal triggering near central Japan from 2000 to 2013. A new time bin declustering method is adopted to remove temporal clustering that can bias tidal triggering estimates. The method bins the seismicity within each cell into 16 equal increments of tidal phase and retains only the maximum size earthquake per phase increment per tidal cycle number. After examining the results for all of the space-time bins with respect to both the semidiurnal and semimonthly tidal phases, we find that the number of bins indicating possible tidal periodicities is no more than might be expected due to random chance and that there is no clear tidal triggering signal prior to the 2011 Tohoku-Oki earthquake.

Acknowledgments

We would like to thank Duncan Angew for synthetic solid Earth tidal strains and helpful comments. The earthquake catalog used in this study is produced by the Japan Meteorological Agency (JMA), in cooperation with the Ministry of Education, Culture, Sports, Science and Technology. The catalog is based on seismic data provided by the National Research Institute for Earth Science and Disaster Prevention, the JMA, Hokkaido University, Hirosaki University, Tohoku University, the University of Tokyo, Nagoya University, Kyoto University, Kochi University, Kyushu University, Kagoshima University, the National Institute of Advanced Industrial Science and Technology, the Geographical Survey Institute, Tokyo Metropolis, Shizuoka Prefecture, Hot Springs Research Institute of Kanagawa Prefecture, Yokohama City, and Japan Agency for Marine-Earth Science and Technology. We also thank William Wilcock and an anonymous reviewer for their suggestions to improve this manuscript.

References

Brinkman, B., M. LeBlanc, Y. Ben-Zion, J. T. Uhl, and K. A. Dahmen (2015), Probing failure susceptibilities of earthquake faults using small-quake tidal correlations, *Nat. Commun.*, *6*, 6175, doi:10.1038/ncomms7157.

Chu, R., S. Wei, D. V. Helmberger, Z. Zhan, L. Zhu, and H. Kanamori (2011), Initiation of the great M_w 9.0 Tohoku-Oki earthquake, *Earth Planet. Sci. Lett.*, *308*(3), 277–283.

Cochran, E. S., J. E. Vidale, and S. Tanaka (2004), Earth tides can trigger shallow thrust fault earthquakes, *Science*, *306*, 1164–1166.
Hardebeck, J. L. (2006), Homogeneity of small-scale earthquake faulting, stress, and fault strength, *Bull. Seismol. Soc. Am.*, *96*(5), 1675–1688.
Hartzell, S., and T. Heaton (1989), The fortnightly tide and the tidal triggering of earthquakes, *Bull. Seismol. Soc. Am*, *79*(4), 1282–1286.
Heaton, T. H. (1975), Tidal triggering of earthquakes, *Geophys. J. Int.*, *43*(2), 307–326.
Heaton, T. H. (1982), Tidal triggering of earthquakes, *Bull. Seismol. Soc. Am.*, *72*(6A), 2181–2200.
Kato, A., K. Obara, T. Igarashi, H. Tsuruoka, S. Nakagawa, and N. Hirata (2012), Propagation of slow slip leading up to the 2011 M_w 9.0 Tohoku-Oki earthquake, *Science*, *335*, 705–708.
King, G. C. P., R. Stein, and J. Lin (1994), Static stress changes and the triggering of earthquakes, *Bull. Seismol. Soc. Am.*, *84*(3), 935–953.
Métivier, L., O. de Viron, C. P. Conrad, S. Renault, M. Diament, and G. Patau (2009), Evidence of earthquake triggering by the solid Earth tides, *Earth Planet. Sci. Lett.*, *278*(3), 370–375.
Reasenberg, P. (1985), Second-order moment of central California seismicity, 1969–1982, *J. Geophys. Res.*, *90*(B7), 5479–5495.
Schuster, A. (1897), On lunar and solar periodicities of earthquakes, *Proc. R. Soc.*, *61*(369–377), 455–465.
Shudde, R., and D. Barr (1977), An analysis of earthquake frequency data, *Bull. Seismol. Soc. Am.*, *67*(5), 1379–1386.
Tanaka, S. (2010), Tidal triggering of earthquakes precursory to the recent Sumatra megathrust earthquakes of 26 December 2004 (M_w 9.0), 28 March 2005 (M_w 8.6), and 12 September 2007 (M_w 8.5), *Geophys. Res. Lett.*, *37*, L02301, doi:10.1029/2009GL041581.
Tanaka, S. (2012), Tidal triggering of earthquakes prior to the 2011 Tohoku-Oki earthquake (M_w 9.1), *Geophys. Res. Lett.*, *39*, L00G26, doi:10.1029/2012GL051179.
Tanaka, S., M. Ohtake, and H. Sato (2002a), Spatio-temporal variation of the tidal triggering effect on earthquake occurrence associated with the 1982 South Tonga earthquake of M_w 7.5, *Geophys. Res. Lett.*, *29*(16), 1756, doi:10.1029/2002GL015386.
Tanaka, S., M. Ohtake, and H. Sato (2002b), Evidence for tidal triggering of earthquakes as revealed from statistical analysis of global data, *J. Geophys. Res.*, *107*(B10), 2211, doi:10.1029/2001JB001577.
Tanaka, S., H. Sato, S. Matsumura, and M. Ohtake (2006), Tidal triggering of earthquakes in the subducting Philippine Sea plate beneath the locked zone of the plate interface in the Tokai region, Japan, *Tectonophysics*, *417*(1), 69–80, doi:10.1016/j.tecto.2005.09.013.
Tsuruoka, H., M. Ohtake, and H. Sato (1995), Statistical test of the tidal triggering of earthquakes: Contribution of the ocean tide loading effect, *Geophys. J. Int.*, *122*(1), 183–194.
Vidale, J. E., D. C. Agnew, M. J. Johnston, and D. H. Oppenheimer (1998), Absence of earthquake correlation with Earth tides: An indication of high preseismic fault stress rate, *J. Geophys. Res.*, *103*(B10), 24,567–24,572.
Wilcock, W. S. (2009), Tidal triggering of earthquakes in the Northeast Pacific Ocean, *Geophys. J. Int.*, *179*(2), 1055–1070.